A Real-Time Power Management Strategy for Hybrid Electrical Ships Under Highly Fluctuated Propulsion Loads

Xie, Peilin; Tan, Sen; Bazmohammadi, Najmeh; Guerrero, Josep M.; Vasquez, Juan C.

Published in:
I E E E Systems Journal

DOI (link to publication from Publisher):
10.1109/JSYST.2022.3177843

Publication date:
2023

Document Version
Early version, also known as pre-print

A Real-time Power Management Strategy for Hybrid Electrical Ships under Highly Fluctuated Propulsion Loads

***Abstract*—The increasing demand for improving fuel efficiency of marine transportation has presented opportunities for the development of power management system (PMS). Different from the terrestrial power system, shipboard power system (SPS) contains a large proportion of propulsion loads, which has the characteristics of high dynamics, periodicity, uncertainty, and high dependence on the marine environment. The propulsion load fluctuation induced by sea waves, in-and-out-of water effects, and changeable consumers requirements, may lead to a low power quality and fuel efficiency. And it brings challenges in the development of marine PMS. In addition, the fluctuated load profiles could also be volatile and unpredictable, which makes long-term load forecasting unrealisable and real-time load forecasting essential. To address these issues, a real-time two-layer PMS is proposed for hybrid-powered ship in this paper, that can maintain a high fuel efficiency and a healthy state of charge (SOC) level over the voyage even in extreme sea conditions. To adapt well to the fluctuated and changeable load condition, a novel multi-step load forecasting (MSLF) system is integrated to make accurate load forecasting in a very very short-term time scale (centisecond). Multiple cases studies are conducted under different cases of voyage time, sailing speed, wave conditions and submergence ratios. The results show that the proposed PMS can significantly reduce the power tracking delays, improve the fuel efficiency, and maintain a healthy SOC level.**

***Index Terms*—Equivalent consumption minimization strategy, fuel efficiency, load forecasting, model predictive control, power management system, shipboard power system.**

NOMENCLATURE

β	Propeller loss factor
$\Delta I_{b.max}$	Maximum battery current changing rate
$\Delta n_{dg.max}$	Maximum DG rotational speed changing rate
η_{chg}, η_{dis}	Efficiencies of battery during charging and discharging mode
η_{dg}, η_{uc}	Efficiency of DG, UC
$\hat{x}$	Predicted state variables
$\hat{y}$	Predicted output variables
μ_b, μ_{uc}	Constant penalty value for battery and UC
ω	Rotational speed of DG
ρ	Sea water density
a_0, a_1, a_2, a_3, a_4	Fixed values by curve fitting
C	DG constant loss
C_{uc}	UC capacitance
D	Propeller diameter
ef_b	Equivalent factor of battery
ef_{uc}	Equivalent factor ofUC
F	Wave disturbance
f	Forecasting horizon of VVSTLF
h	Propeller shaft submergence
$I_{b/uc.min}, I_{b/uc.max}$	Minimum and maximum current of battery and UC
I_b	Battery current
I_{uc}	UC current
k_c	DG copper loss coefficient
k_i	DG iron losses coefficient
K_Q	Torque coefficient
K_T	Thrust coefficient
k_w	DG windage losses coefficient
k_b, k_{uc}	Penalty coefficient of battery and UC
m	Total mass of ship
m_b	Equivalent fuel consumption of battery
m_{dg}	DG fuel consumption
m_{total}	Total equivalent fuel consumption
m_{uc}	Equivalent fuel consumption of UC
N_c	Control horizon
N_p	Prediction horizon
$n_{dg.min}, n_{dg.max}$	Minimum and maximum rotational speed of DG
n_{dg}	Diesel engine speed
n_{prop}	Propeller motor shaft speed
p, d, q	Estimated load model orders
P_b	Output power of battery
P_{dg}	DG output power
P_{eng}	Output power of the diesel engine
P_{load}	Propulsion load
P'_{load}	Forecasted load by VVSTLF
P_{loss_b}	Power loss of battery
$P_{loss_{dg}}$	DG total loss
$P_{loss_{uc}}$	Power loss of UC
P_{uc}	Output power of UC
Q_b	Battery capacity
Q_{prop}	Propeller torque
R_F	Ship frictional resistance
R_W	Wave-making resistance
R_{air}	Air resistance of ship
R_b	Internal resistance of battery
R_{uc}	Internal resistance of UC
$s_{b.min}, s_{b.max}$	The minimum and maximum battery SOC
s_b	SOC of battery
$s_{uc.min}, s_{uc.max}$	Minimum and maximum UC SOC
s_{uc}	SOC of UC
$SFOC_{eq}$	Equivalent value for the virtual fuel consumption
T	DG engine torque
t_d	Thrust deduction coefficient
T_f	DG friction losses coefficient
T_{prop}	Propeller thrust
U	Ship speed
u	Control inputs

u^*	Optimal control inputs
V_{oc}	Open-circuit voltage of the battery
V_{uc}	Maximum voltage of UC
x	State variables
y	Output variables
AR	Auto-regressive
ARIMA	Auto-regressive integrated moving average
DG	Diesel generator
ECMS	Equivalent consumption minimization strategy
EF	Equivalence factor
ESS	Energy storage systems
HESS	Hybrid energy storage system
LP	Linear prediction
LR	loss reduce
MA	Moving average
MPC	Model predictive control
MSLF	Multi-step load forecasting
PMS	Power management systems
SFOC	Specific fuel oil consumption
SPS	Shipboard power systems
STLF	Short-term load forecasting
UC	Ultra-capacitor

I. Introduction

TRANSPORTATION industry is currently becoming the foundation of national economy, where marine transportation takes 80% of world's trade. However, due to the widespread use of fossil fuels, marine fleet becomes a large contributor to greenhouse gasses and other emissions. According to the International Maritime Organization (IMO), who has set an ambition to reduce the carbon intensity of emissions from shipping by at least 40% by 2030, and 70% by 2050, compared with 2008 levels, effort should be made to accelerate decarbonization [1].

Two main approaches can be conducted to achieve that, including improving the fuel efficiency of traditional fuel-consumed gensets and utilizing alternative low-carbon fuels instead (such as wind, photovoltaic panel, biodiesel, algae, liquid natural gas, hydrogen [2], etc.). Although alternative fuels can achieve lower or even zero emission than conventional fuels, they are still rare in applications and the corresponding research is quiet new and needs further development. In addition, while under changeable marine environment, disadvantages such as low power quality, insufficient sustainability, unpredictable generation behavior may bring extra challenges especially in the areas of sizing, generation forecasting, energy management, and typologies designing. Considering the fact that currently more than 95% of ships still use diesel engines as the main power source, improving the efficiency of traditional fuels is more urgently needed and is the main concern in this paper. One way to improve the fuel efficiency is to replace the traditionally commonly used fixed-speed DGs with variable-speed DGs. By allowing the diesel engines varying within a specific range, an average fuel savings in the range of 10% to 20% can be expected [3]. In addition, effectiveness of energy storage system (ESS) has been proved in enhancing the system stability, power quality, operation flexibility, and energy efficiency [4], [5]. However, the mix use of the different types of energy sources, that includes traditional gensets and different kinds of ESSs may increase the complexity of the shipboard power system and thus require power/energy management strategies (PMS/EMS) to enable economical and environmental friendly operations.

Although PMS has been developed in many other areas viz. terrestrial [6], vehicle, and aircraft power systems, new challenges arise for SPS. One of the main differences between them is the composition of loads. In marine applications, ship propulsion load takes a large part of the onboard loads, which is affected largely by the environment, especially the sea states. In extreme sea conditions, propulsion loads can be severely fluctuated due to ventilation and propeller in-and-out-of water effects [7]. If not handled well, there will be negative impacts on both electrical and mechanical shipboard system, such as increased fuel consumption, risk of blackouts due to unpredictable power consumption, and increased maintenance cost due to unnecessary mechanical wear and tear [8]. As a result, research efforts on dealing with high dynamic loads, coordinating multiple power sources, and maintaining high fuel-efficiency operation is an urgent need.

A. State of the Art

To address the aforementioned problem of highly fluctuated propulsion loads, efforts can be made including: designing thruster controllers for power smoothing [8], [9], and hybrid using of energy storage system (HESS) [10]–[14] for power fluctuation compensation. Among the latter publications, different hybrid ESS use are introduced and recommended. For example, [11], [12] proposed the hybrid combination of batteries and UCs, where UCs supply pulse or high-frequency loads and batteries provide auxiliary for the main power supplier. Further in [11], the parameter uncertainty of the utilized HESS was studied and identified online to mitigate load fluctuations and improve the system efficiency. While in [10], UC is replaced with a flywheel due to its higher power density and higher energy density. Results in these work all indicate that the hybrid use of ESS can meet the requirement of high dynamic load demands while avoiding frequent charging and discharging of batteries, reducing mechanical and electrical losses, extending service life and providing good power tracking ability under different sea states. Therefore in this paper, the hybrid use of batteries and UCs is utilized.

However, effectiveness of the HESS depends largely on the power management strategy, which decides the way of power splitting between main gensets and hybrid ESS according to different optimization goals.

Research in marine PMS/EMS can be generally classified into global planning and real-time scheduling [5]. The former requires knowledge of the entire system and has the ability to acquire the global optimal decision. It is useful in solving the problems of facility sizing, early-stage energy dispatching, and ship routine scheduling in a financial and green way, however may requires long-term of past data, wide perspectives of knowledge, and large computational efforts. Thus, it is usually conducted offline and ahead of time. On the contrary, the

latter uses instantaneous measured data to provide real-time guidance, and is more suitable in dealing with uncertainties and dynamic situations.

Corresponding real-time power management strategies developed in the aforementioned papers all show good performance in allocating power between hybrid energy resources. Some are targeted to minimize the electrical losses [10]–[13] while some minimize the fuel consumption [14]–[16]. However, one of the major concerns and also the drawback of the real-time PMS is the lack of long-term perspectives. All the previous work only focuses on the instant power splitting according to the current load and generation situation, but may not guarantee a healthy state of charge (SOC) level of HESS throughout the voyage. Given the fact that, the propulsion loads would show different characteristics under different sea states, ship sailing speed, and voyage conditions, and would vary largely at ship departure, accelerating, sailing, and arriving [17], [18]. The highly changeable propulsion load in addition with the volatile environment and uncertainty at sea, all require a sufficient energy backup to maintain system stability and safety [19]. Therefore, guaranteeing a healthy SOC level of HESS, is of great importance to ensure a continuous energy supply and is one of the major concerns in this paper. To do that, a two-layer PMS structure combining real-time optimization PMS together with rule-based algorithms is developed.

To improve the performance of PMS, better knowledge of future loads is necessary, which makes propulsion load estimation and forecasting worthwhile.

Current load forecasting methods can be generally classified into machine-learning-based methods and statistical methods [20]. The former requires large historical information and is more suitable for regular or seasonable offline load forecasting. While the latter extracts useful modeling parameters and is more popular in short-term time series analysis. Most of the current studies on marine load forecasting stick on the long-term time horizon and the results are mostly used for supporting global-planning targets such as optimal size designing and early-stage energy dispatching [21]–[24]. Corresponding studies on real-time scheduling is much less. However, today model predictive control (MPC) has been widely used to solve the real-time power allocation problem [25]–[28], expected to improve the overall performance by allowing the system to look several steps ahead. Most work simply consider the average or fixed load value during the MPC prediction horizon [28], [29]. One major concern is that MPC would perform nicely if only the load condition does not change too much during the prediction horizon. While under high fluctuated load condition, the lack of future step's load information would largely debilitate the performance of the MPC, and therefore result in wasted computing effort. Some work, on the other hand, addresses this problem by propulsion load modeling [30]–[32]. However, the mathematical model would only be valid for a certain sea states and may loss its accuracy under different sea conditions or propeller submergence ratio. And in [33], linear prediction with input observer is adopted based on the mathematical model. However, due to the inherent limit of linear prediction, it is one-step accuracy only and may not meet the requirement of MPC with multiple prediction steps. To meet all load types with zero prior knowledge of future information, and to acquire multi-step accuracy, an intelligent method, Double Q reinforcement learning, is used in [34]. However, such method requires more historical load information, longer computing effort, and might be difficult for real-time application and highly fluctuated conditions. Therefore, an applicable multi-step load forecasting method is needed to assist MPC for better performance, and is another major concern in this paper.

B. Objectives and Contributions

To address the above challenges, this paper proposed a real-time PMS framework together with a multi-step load prediction system to decide the optimal power split between multiple energy sources with two objectives: (i) a healthy SOC level of HESS throughout the whole voyage. (ii) to ensure fuel-efficient generator operation. The main specific contributions of this paper are:

1) A two-layer PMS for SPS: A two-layer PMS frame is developed in this paper. The outer-layer is rule-based, scheduling the on/off status of DG to ensure the SOC of HESS at a tolerable level and avoid low-load operation of DG. Given the knowledge of the operation condition of DG from the outer-layer, the inner-layer is optimization-based, solving the equivalent consumption minimization problem to decide the most fuel-efficient way of power splitting and to maintain the SOC at a healthy level at the same time.

2) Multi-step load forecasting: Due to the advantages in fast computing speed, high prediction accuracy, and capability of multi-step forecasting [35], auto-regressive integrated moving average (ARIMA) is utilized here to develop a real-time multi-step load forecasting (MSLF) system. The proposed MSLF is integrated in the inner-layer to predict the future load in ahead of multiple steps. Different from the previous load forecasting methods which either have a long-term time scale or one-step accuracy only, the proposed MSLF has a very short-term time scale and is capable of providing multiple-step prediction while maintaining good accuracy. Integrated with MPC, the proposed MSLF helps to update the load information at every prediction step, thus offering the possibility of improved power tracking ability and wiser power distribution decision.

C. Paper Organization

This paper is organized as follows. In Section II, the hybrid powered SPS model and ship hydrodynamic model are presented. The proposed two-layer real-time PMS is developed in Section III. In section IV, comprehensive simulations are provided to validate the effectiveness of the proposed PMS by multiple cases studies. Finally, the conclusions are given in Section V.

II. SPS Description and Modeling

The basic components of a SPS studied in this paper consist of HESS (batteries and ultra-capacitors), variable-speed DG,

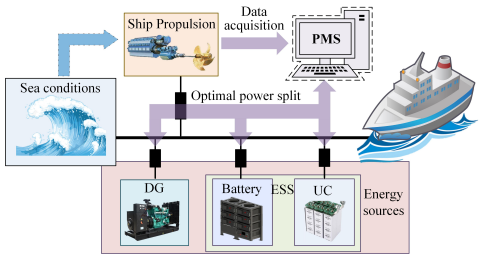

Fig. 1: General structure of shipboard power system

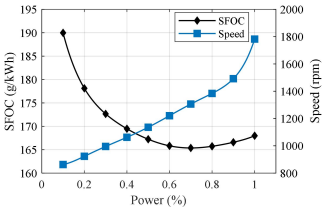

Fig. 2: SFOC,n_{dg}versus P_{eng}

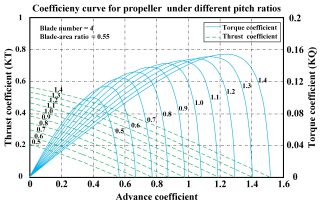

Fig. 3: Propeller coefficiency

and propulsion load, as shown in Fig. 1. HESS is able to alleviate energy management difficulties by adjusting the charging/discharging status; DG is utilized to provide stable energy to meet the requirement of propulsion load demand. As shown, a SPS can be considered as a typical islanded microgrid, but with large dynamic loads and multiple power sources. The PMS acts as a coordinator between them, collects information on past and current loads, predicts future loads, and determines the optimal power allocation to maintain good fuel efficiency, power quality, and SOC level.

A. Modeling of Diesel Generator

Due to the potential of higher fuel efficiency, variable-speed DG is utilized here as the main power supplier. The characteristics of optimal specific fuel oil consumption (SFOC) and optimal operational point of variable-speed DG are shown in Fig. 2 [36], [37]. As seen from the blue line, the optimal operational speed is different under different load conditions. And the corresponding SFOC values under different loads are presented by black line. DG tends to acquire a low fuel efficiency at low load condition. Therefore, to obtain a high fuel-efficiency operation, it is better for the generator to operate at high load condition. The output power of the diesel engine (P_{eng}) can be expressed as a nonlinear function of engine speed (n_{dg}), with a_0, a_1, a_2, a_3 fixed values by curve fitting as,

$$P_{eng} = a_0 + a_1 n_{dg} + a_2 n_{dg}^2 + a_3 n_{dg}^3 + a_4 n_{dg}^4 \tag{1}$$

Here a_0, a_1, a_2, a_3, a_4 are fitted as $-1.93 \times 10^7, 5.7098 \times 10^4, -63.97, 0.0333, -6.5138 \times 10^{-6}$ respectively. And the SFOC is also formulated as:

$$SFOC = \begin{cases} b_0 + b_1 n_{dg} + b_2 n_{dg}^2 + b_3 n_{dg}^3 \\ \quad + b_4 n_{dg}^4 + b_5 n_{dg}^5 + b_6 n_{dg}^6 & n_{dg} <= 1340 \\ c_0 + c_1 n_{dg} + c_2 n_{dg}^2 & n_{dg} > 1340 \end{cases} \tag{2}$$

where $b_0, b_1, b_2, b_3, b_4, b_5, b_6$ are fitted as $2.12 \times 10^4, -100.30, 0.20, -2.08 \times 10^{-4}, 1.22 \times 10^{-7}, -3.78 \times 10^{-11}, 4.83 \times 10^{-15}$ and c_0, c_1, c_2 are fitted as $136.13, 0.03, -8.81 \times 10^{-6}$.

The diesel engine provides torque to the generator, the generator converts that torque into electrical energy. The losses of this process majorly conclude: copper losses (k_c), iron losses (k_i), friction losses (T_f), windage losses (k_w) and constant losses (C) [38]. Therefore, total losses ($P_{loss_{dg}}$) can be represented as a nonlinear function of engine torque (T),

$$P_{loss_{dg}} = k_c T^2 + k_i \omega + T_f \omega + k_w \omega^3 + C \tag{3}$$

Once the losses have been determined, the output power of the diesel generation system (P_{dg}) can be derived as,

$$P_{dg} = P_{eng} - P_{loss_{dg}} \tag{4}$$

B. Hybrid Energy Storage System

Owing to the advantage in high energy density, ultra-capacitors (UCs) are able to deliver energy faster than batteries, thus capable of supplying high frequency load. However, the energy capacities of commercially available UC are smaller than the same size of batteries [39]. From the perspective of security and economy, batteries and UCs hybrid ESS is utilized in this paper. The state-space equation of HESS can be defined as [13],

$$\begin{bmatrix} \dot{s_b} \\ \dot{s_{uc}} \end{bmatrix} = \begin{bmatrix} -1/(3600 Q_b) & 0 \\ 0 & -1/(V_{uc} C_{uc}) \end{bmatrix} \begin{bmatrix} I_b \\ I_{uc} \end{bmatrix} \tag{5}$$

where s_b, s_{uc} are the SOC of the battery and UC, I_b and I_{uc} are the currents, Q_b is the battery capacity, V_{uc} is the maximum voltage of UC, C_{uc} is the UC capacitance.

Taking the power losses into account, the terminal power of battery (P_b) and UC (P_{uc}) can be expressed as follows,

$$P_b = V_{oc} I_b - P_{loss_b} = V_{oc} I_b - R_b I_b^2 \tag{6}$$

$$P_{uc} = V_{uc} s_{uc} I_{uc} - P_{loss_{uc}} = V_{uc} s_{uc} I_{uc} - R_{uc} I_{uc}^2 \tag{7}$$

where V_{oc} is the open-circuit of the battery, which is assumed to be constant and equal to the DC bus voltage. P_{loss_b} and $P_{loss_{uc}}$ are the power losses caused by internal resistance R_b and R_{uc} respectively.

C. Propeller and Ship Hydrodynamic

The propulsion load of the ship can be derived from the propeller model and the hydrodynamic model. The propeller thrust (T_{prop}), torque (Q_{prop}) and mechanical power (P_{load}) can be formulated as nonlinear functions of motor shaft speed (n_{prop}), environmental parameters (e.g. water density (ρ), wave period), and propeller parameters (e.g. propeller diameter (D), pitch ratio, submergence (h)). And it can be expressed as [40],

$$T_{prop} = sign(n_{prop}) \beta \rho n_{prop}^2 D^4 K_T \tag{8}$$

$$Q_{prop} = sign(n_{prop}) \beta \rho n_{prop}^2 D^5 K_Q \tag{9}$$

$$P_{load} = 2\pi n_{prop} Q \tag{10}$$

where K_T and K_Q are determined by advance coefficient, pitch ratio, expanded blade-area ratio and number of blades. The relationships between them are shown as Fig. 3. And the details can be found in reference [41]. β is the propeller

loss factor, referring to the effects of propeller in-and-out-of water motion and is sensitivity to submergence ratio (h/D), expressed as [7], [42],

$$\beta = \begin{cases} 0 & h/D < -0.48 \\ 1 - 0.675 \times (1 - h/D)^{1.258} & -0.48 \leq h/D \leq 1.3 \\ 1 & h/D > 1.3 \end{cases} \tag{11}$$

As seen from (8)-(11), the propeller submergence ratio is the main reason for the high-frequency fluctuation of the propulsion load. Different submergence condition will result in different types of load fluctuation. This paper tests three different types of submergence conditions. Details will be shown in Section IV.

The presented propeller and ship hydrodynamic models provide the foundation for simulating real-time propulsion loads. Extreme conditions are tested where the high-frequency fluctuation is up to 10 Hz due to the in-and-out-of water behavior of propeller, and the low-frequency fluctuation is at around 0.1 Hz due to wave disturbance. To reduce the negative effects of it, the proposed PMS is presented in Section III.

III. Power Management Strategy for SPS

In this paper, a real-time two-layer power management strategy is proposed for SPS. The overall objective is to acquire a high fuel-efficiency operation as well as maintain a healthy level of SOC to guarantee a continuous service basis. The overall PMS structure is shown in Fig. 4. The outer-layer is rule-based, adjusting the on/off status of DG according to the information of current SOC and the propulsion load condition. The aim is to keep the SOC within hard constraints (10%-95%) while maintaining the DG at a relative high efficiency point. And the inner-layer is optimization-based, containing two parts: multi-step load forecasting system (MSLF) and optimization system. By collecting the load information from past several minutes, MSLF is able to predict future load for the next few steps. With the future load information from MSLF, current system states, and the DG on/off signal from the outer-layer, optimization system decides the optimal power split between the energy sources with the aim of highest fuel efficiency and healthy SOC level under soft constraints (40%-90%).

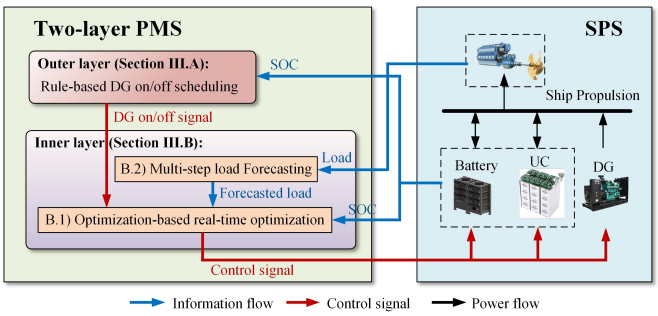

Fig. 4: Overall structure of the proposed PMS

A. Rule-based outer layer PMS

Based on the status of the SOC, and the current on/off status of DG, the next step´s on/off decision will be determined by the following rules:

i. Initialization: DG is off
ii. If the lower SOC threshold (10%) is reached or the load reaches its maximum threshold, then,:
   - DG is on
iii. If the upper SOC threshold is reached (95%), then,:
   - DG is off
iv. Goto ii and loop

The maximum threshold here is typically set to the maximum output power limit of batteries for the consideration of battery lifespan and the continuity of power supply. This process ensures that the HESS will not be overcharged or overdischarged by managing the on/off of DG, and it also prevents the DG from low-load operation. As from Fig. 2, DG tends to acquire lower fuel-efficiency at low load conditions, thus higher fuel efficiency can be maintained through this process. The on/off signal k_{dg} is then sent to the next layer. k_{dg} is a logical variable, with 0 denoting off and 1 standing for on.

B. Optimization-based inner layer PMS

A high fuel-efficiency power split will not be achieved only with the outer-layer. For the purpose of obtaining the optimal power distribution and a healthy level of SOC, the inner-layer is developed.

The formulation of the optimization problem is based on ECMS, an effective energy management technique capable to minimize the fuel consumption. The basic concept of ECMS is that the ESS can be seen as auxiliaries for the DG. By regulating the charging/discharging of ESS according to the SOC condition and current load demand, DG can be maintained at a high fuel-efficiency point. It calculates the instantaneous equivalent fuel consumption of energy storage systems and determines the optimal power split with low computational burden and limited calibration of control parameters [43].

The cost function of ECMS is the combination of fuel consumption of DG and equivalent fuel consumption of HESS [44]. The accuracy depends on the equivalence factor (EF), which stands for the conversion relationship between the electrical power consumption and fuel consumption. Thus, it needs to be carefully considered. Most of researches simply considered the EF as a constant [45]. Although easily to be implemented in real time, it may fail to capture the real transformation relationship, thus lead to unsatisfying results. So, in this paper, the EF is adjusted in real-time according to the current SOC conditions. Although it may require more computational effort, more accurate equivalent fuel conversion ability can be expected.

1) ECMS-based Problem Formulation: The total equivalent fuel consumption (m_{total}) is the sum of generator fuel consumption (m_{dg}), and converted equivalent fuel consumption of battery (m_b) and UC (m_{uc}),

$$m_{total}(t) = k_{dg} \cdot m_{dg}(t) + m_b(t) + m_{uc}(t) \tag{12}$$

where m_{dg} can be calculated by,

$$m_{dg}(t) = SFOC \cdot P_{dg}(t)/(\eta_{dg} \cdot 3.6 \cdot 10^6) \quad (13)$$

with η_{dg} be the diesel generator efficiency. m_b and m_{uc} can be expressed as follows,

$$m_b(t) = ef_b(t) \cdot SFOC_{eq} \cdot P_b(t)/(3.6 \cdot 10^6) \quad (14)$$

$$m_{uc}(t) = ef_{uc}(t) \cdot SFOC_{eq} \cdot P_{uc}(t)/(3.6 \cdot 10^6) \quad (15)$$

where ef_b and ef_{uc} are equivalence factors of battery and UC. $SFOC_{eq}$ sets a reference fuel consumption value for the HESS. Noticed that if the equivalent fuel cost $SFOC_{eq}$ is tuned too low, HESS is encouraged to be charged, because the energy in the HESS is considered cheaper than DG. A value that is too high will discourage battery use because of high recharge costs. Considering the additional transfer and conversion losses during the charging/discharging process and the high fuel-efficiency characteristic of variable-speed DG under high load conditions, the $SFOC_{eq}$ here is set as the peak consumption value of SFOC in Fig. 2 such that it can encourage the DG to take on more power, thus avoiding low load operation.

The equivalence factors of battery ef_b can be derived as [46],

$$ef_b(t) = \begin{cases} \dfrac{k_b}{\eta_{dg} \cdot \eta_{dis}} & P_b \geq 0 \\ \dfrac{k_b \cdot \eta_{chg}}{\eta_{dg}} & P_b < 0 \end{cases} \quad (16)$$

where η_{chg} and η_{dis} are constant values, which refer to the average efficiencies of battery during charging and discharging mode, respectively, and both set as 0.95 in this paper. k_b is the penalty coefficient of battery. The key point of it is to keep the SOC varies around a healthy level ($s_{b.min} \sim s_{b.max}$), and is expressed as,

$$k_b = 1 - \mu_b \frac{s_b - (s_{b.min} + s_{b.max})/2}{(s_{b.min} + s_{b.max})/2} \quad (17)$$

where μ_b is a constant value, standing for the penalty of SOC when it deviates from the baseline ($\frac{1}{2}(s_{b.min} + s_{b.max})$). A value that is too high would encourage the battery to stick to the specified SOC level, however discourage it from engaging in charging or discharging. Conversely, a value that is too low will allow more liberal charging and discharging behavior, but may result in larger SOC deviation. To obtain a better ability of supporting the main DG while maintaining a healthy SOC level at the same time, here μ_b is set as 1.2 after a trade-off. $s_{b.min}$ and $s_{b.max}$ represent the lower and upper limits of SOC and is set as 30% and 90% respectively. The penalty coefficient k_b varies with the change of SOC state and can effectively limit the SOC under soft constraints. For example, when the battery is in discharging mode, SOC decreases. And as the SOC deviates from the limit, k_b increases, resulting in a decrease in battery discharging power. Therefore a healthy SOC condition is maintained. However, it should be noted that different from the hard constraints in the outer-layer, the limits here is soft and can be violated at extreme load conditions. The presence of the dual constraints regulates the operation of DG and HESS, to guarantee a healthy level of SOC and reliable energy backup.

As for ef_{uc}, similar equation is held except that the μ_{uc} is much greater than batteries. The main reason of a larger μ_{uc} is that larger ef_{uc} results in larger penalty for the deviation from the mid-point SOC value. So the UC will be considered more expensive and supply the high-frequency load only. But UC can still provide auxiliary to the battery and DG by supporting low-frequency load while under extreme load conditions (eg: change load condition, extreme high or low load condition), which enables a more flexible operation.

From the above analysis, the total equivalent fuel consumption is obtained instantaneously. The optimization problem is integrated with MPC to make real-time power splitting decision. MPC is based on the system discretized model. A sequence of future system states and outputs can be predicted by,

$$\hat{x}(t_{k+N_p}) = f(x(t_k), u(t_{k+1}), \cdots, u(t_{k+N_c})) \quad (18)$$

$$\hat{y}(t_{k+N_p}) = g(x(t_k), u(t_{k+1}), \cdots, u(t_{k+N_c})) \quad (19)$$

where $x(t_k) = [P_{dg}(t_k), s_b(t_k), s_{uc}(t_k)]^T$, denotes the state variables, $y(t_k) = [P_{dg}(t_k), P_b(t_k), P_{uc}(t_k)]^T$ is the output variables, $u(t_k) = [n_{dg}(t_k), I_b(t_k), I_{uc}(t_k)]^T$ is the control inputs. N_p is the prediction horizon. N_c is the control horizon, and is set as 1 in this paper.

The optimization target is to reduce the total fuel consumption in real time, therefore the cost function at time t_k is formulated as,

$$\min_{u(t_j)} \quad J = \sum_{j=k}^{k+N_p-1} m_{total}(t_j) \quad (20)$$

with a set of equality and inequality constraints,

$$\begin{aligned} s.t. \quad & k_{dg} \cdot P_{dg}(t_j) + P_b(t_j) + P_{uc}(t_j) = P'_{load}(t_j) \\ & n_{dg}(t_j) \in [n_{dg.min}, n_{dg.max}] \\ & I_{b/uc}(t_j) \in [I_{b/uc.min}, I_{b/uc.max}] \\ & \Delta n_{dg} \leq \Delta n_{dg.max} \\ & \Delta I_b \leq \Delta I_{b.max} \end{aligned} \quad (21)$$

where the P'_{load} is the predicted load from the MSLF system. The equality constraint ensures that the load demand is met at every prediction step. And the inequality constraints govern the rotation speed limits of the variable-speed DG, the currents limits of HESS, and the limits of changing rate of them. Subscript min and max refers to the lower and upper limit, and the Δ stands for the changes within a sampling time. Detailed data is shown in Tab. I.

TABLE I: Optimization constraints

Parameters	Symbol	Value
DG rotational speed lower limit	$n_{dg.min}$	900 rpm
DG rotational speed upper limit	$n_{dg.max}$	2000 rpm
Battery current lower limit	$I_{b.min}$	-300 A
Battery current upper limit	$I_{b.max}$	300 A
UC current lower limit	$I_{uc.min}$	-800 A
UC current upper limit	$I_{uc.max}$	800 A
DG rotational speed changing limit	$\Delta n_{dg.max}$	10 rpm/s
Battery current changing limit	$\Delta I_{b.max}$	20 A/s

2) Multi-step Load Forecasting: Extreme sea conditions are tested in this paper where the ship propulsion load is highly periodical and varies rapidly with the frequency up to 10 Hz. Therefore, the sampling time here is set as 0.01 s. During a short time period, the propulsion load can be modeled as an ARIMA model and accurately predicted within dozens of steps. ARIMA indicates that the time series is regressed on its own past data and the forecast error is a linear combination of past respective errors [47]. Thus, the predicted value is differenced in the degree of d, and is the sum of auto-regressive (AR) part and moving average (MA) part with p be the order of AR part and q be the order of MA part.

For the estimation of the propulsion load model p, d, q , method in [48] is utilized with the collection of the load information from the past few seconds. Thus the future T steps ($T > N_P$) can be predicted. The overall signal flow chart of the inner-layer PMS is shown in Fig. 5. The MSLF collects load information from the past few seconds for load estimation and predicts the future T steps all at once. Then, the predictions are sent to the optimization part sequentially in the order of N_p per step, until all the predicted data are run out. And the MSLF is reactivated and continues to predict another next T steps with the latest load information.

The overall control structure of the inner-layer PMS is shown in Fig. 6. The MSLF predicts the propulsion load for the next few steps. The MPC-based optimization system calculates the future system states, adjusts the future equivalence factors, and solves the optimization problem based on the on/off status of DG from outer-layer and the forecasted load data sent from the MSLF part. By allowing the load information updated in next and next few steps, MPC is able to solve the optimal power splitting problem while taking full consideration of future load trends, which enhances the fuel saving potential and avoids the power tracking delays caused by the sampling and calculations.

Compared to the traditional most commonly used LP method, which stays a high accuracy when predicting for one step ahead but can be extremely inaccurate if it predicting for more steps, the proposed MSLF is able to predict for tens of steps ahead while maintaining a high accuracy as seen from Fig. 7 and Fig. 8. Fig. 7 - 8 give the prediction performance of MSLF and LP at one-step length prediction and multiple-step length respectively. It can be observed from Fig. 7 that the MSLF can acquire a comparable high accuracy as LP when both predicting for only one step. While in Fig. 8, the accuracy of MSLF decreases as the forecasting horizon

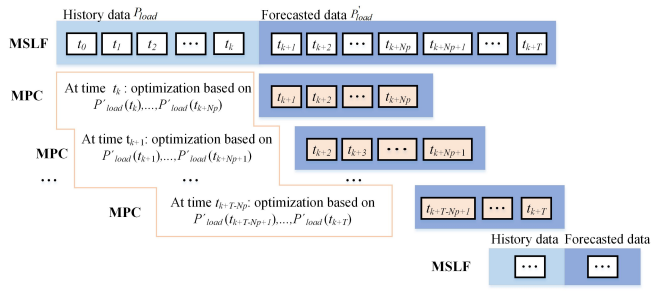

Fig. 5: Signal flow chart of the inner-layer PMS

increases, however, LP becomes extremely inaccurate when predicting for over-one step.

In conclusion, there is a trade-off in the determination of MSLF forecasting horizon. A longer forecasting horizon indicates less computational efforts but at the same time brings a lower accuracy. Conversely, a shorter forecasting horizon requires higher-frequency forecasts but guarantees more accurate returns. In this paper, to maintain a relatively high accuracy as well as less computational efforts, the forecasting horizon T is set as 20 steps.

Due to the nonlinear relationship brought by DG model and ECMS model, the optimization problem formulated here is nonlinear and is solved by fmincon program in MATLAB.

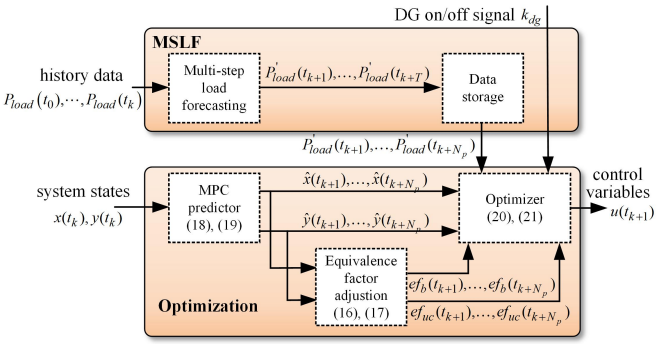

Fig. 6: Overall control structure of the inner-layer PMS

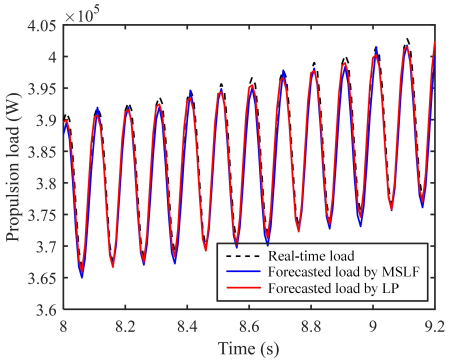

Fig. 7: Forecasting performance of MSLF and LP when both predicting only one step

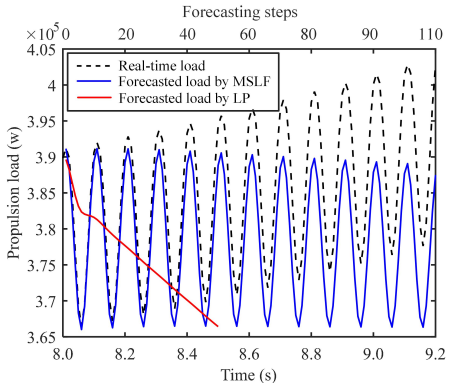

Fig. 8: Forecasting performance of MSLF and LP when both predicting for multiple steps ahead

TABLE II: Ship and hydrodynamic parameters

Parameters	Symbol	Value
Water density	ρ	1.025 g/cm^3
Number of blades	Z	4
Propeller diameter	D	5.6 m
Ship mass	m	2×10^4ton
Added mass	m_x	3×10^4 ton
Thrust deduction coefficient	t_d	0.2s
Frictional resistance coefficient	C_f	0.0043
Wave-making resistance coefficient	C_W	0.0043
Wind resistance coefficient	C_{air}	0.8
Ship wetted area	S	12300 m^2
Advance facing area in the air	A_t	675 m^2

TABLE III: Electrical parameters.

Modules	Parameters	Symbol	Values
Diesel Generator	Rated power	P_d^*	2 MW
	Efficiency	η_d	96%
Battery	Rated power	P_b^*	37.5 kW
	Capacity	Q	300 Ah
	SOC Range	$s_{b.min/max}$	0.2, 0.9
	Initial SOC	s_{init}	0.5
Ultra-capacitor	Rated power	P_u^*	25 kW
	Capacitance	C_u	63 F
	Resistance	R_u	6.8 mΩ
	SOC Range	$s_{u.min/max}$	0.2, 0.9
	Initial SOC	s_{init}	0.5

IV. Simulations and Results Analysis

To evaluate the performance of the proposed PMS, several cases studies are conducted. Tab. II demonstrates all the ship and hydrodynamic parameters [12]. The power sources on board mainly consist of a diesel generator, 8 sets of batteries and 10 sets of UCs. The parameters of each power module are listed in Tab. III. The sampling time is 0.01 s. The main purposes of the cases studies are to illustrate the benefits of the proposed PMS by comparing the power tracking ability, fuel savings, and the SOC levels. Multiple sailing conditions and sea states are tested under two different cases: short-time sailings with constant speed under different sea states; and a long-time voyage including departure, accelerating, navigation and arriving. In addition, to evaluate the effectiveness of the proposed PMS scheme, traditional used LR-based method as in [10]–[13], and the previously used ECMS method as in [14] are used as benchmarks.

A. Cases Description

1) Short-time constant speed sailings: According to the ship hydrodynamic model, the propulsion load is effected largely by the sea states and the propeller submergence ratio. Due to the different types of submergence ratio of the propeller, the propulsion load shows different characteristics. To test the performance of the proposed PMS, extreme sea conditions are studied where the sea wave frequency is up to 0.1 Hz and the propeller in-and-out-of water frequency is up to 10 Hz. Three load conditions are tested including: regular load condition, noisy load condition, and high-submergence ratio condition.

For regular load condition, the propeller submergence ratio is modeled as an ideal sinusoid [49],

$$h/D = 1.2 + 1.2\cos(\frac{2\pi}{0.1}t) \tag{22}$$

where t is the time. The propulsion load curve when the ship is at a constant high vessel speed of 6.2 knots is shown in Fig. 9. As seen, the load curve is a sinusoid wave with two different frequency, the low frequency is 0.1 Hz and high frequency is 10 Hz, caused by sea wave and propeller in-and-out-of-water behavior respectively.

However in practice, the propulsion load will not exhibit the desired sinusoidal properties. Due to the existence of small ripples, trembles of propeller submergence, and small disturbances from the nature, noises are added to the original load waveform to mimic the real loads as in Fig. 10.

For ships with a high propeller submergence ratio, but not fully submerged, the propeller loss factor (β), which denotes the propeller in-and-out-of water effect, will be like a flat-topped sinusoidal wave as in Fig. 11. The data is obtained by curving fitting from [50]. Corresponding propulsion load is shown in Fig. 12. As seen, due to the effect of the propeller submergence ratio, the high-frequency fluctuation of the propulsion load also exhibits a flat-topped characteristic.

To test the performance in power tracking capability due to the integration of the proposed MSLF, Fig. 13-15 give the comparisons of power tracking performance between non-MSLF integrated PMS and MSLF integrated PMS when the ship is at a constant high speed (6.2 knots) under the three sea submergence conditions, respectively. Load forecasting results under the three sea conditions indicate that good prediction accuracy can be achieved in all the three cases tested, while the highest accuracy is obtained in the ideal normal condition. And by comparing the load tracking performance between the proposed PMS with and without MSLF, it can be seen that MSLF can effectively avoid power tracking delays caused by sampling, thus improve the power tracking capability.

2) Long-time variable speed sailings: The ship propulsion load depends not only on the sea state, but also on the ship operation mode. To test the effectiveness of the proposed PMS under different vessel operational conditions, a full one-hour cruise consisting of four modes of operation is studied here, including accelerating, high-speed navigation, decelerating, and low-speed sailing. Ship operation conditions and load profiles of this one-hour cruise are developed based on the data from [51]. Fig. 16 shows the curves of the one-hour load demand, power splitting between the onboard gensets, and the SOC status of HESS respectively. During the first 15 minutes, the ship departures from the port and accelerates from 0 to 12 knots. Then after around half an hour high-speed navigation, accompanied with occasional speed changes, the ship returns to the port at the last 15 minutes. Through the whole voyage, the propulsion load is fluctuated heavily, showing the same characteristics as normal condition as discussed in the last subsection.

It can be observed that the propulsion load could be very low at the beginning and the end of the voyage, varying in the range of 0 to 2 MW. During the first 5 minutes, the propulsion

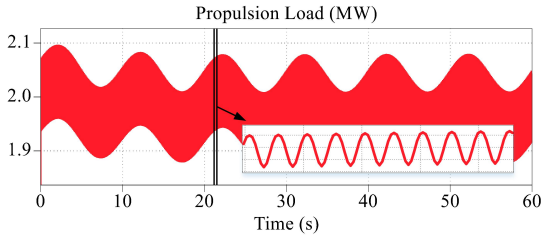

Fig. 9: Normal propulsion load

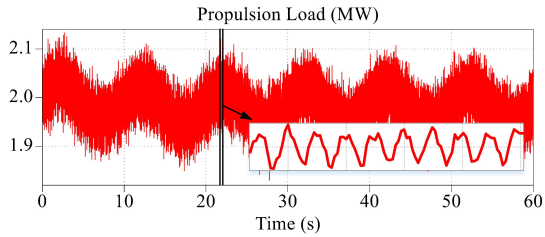

Fig. 10: Noisy propulsion load

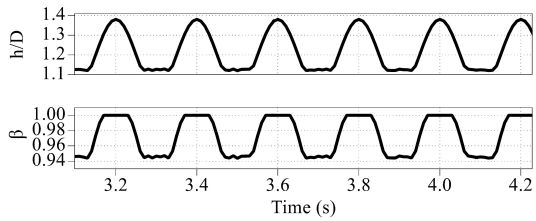

Fig. 11: Propeller submergence ratio and loss factor

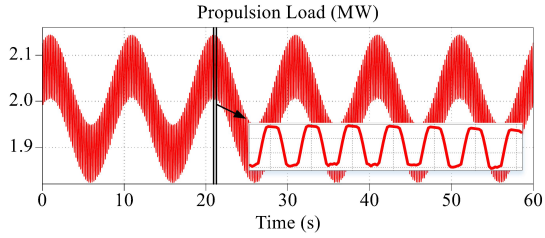

Fig. 12: Propulsion load under high submergence ratio

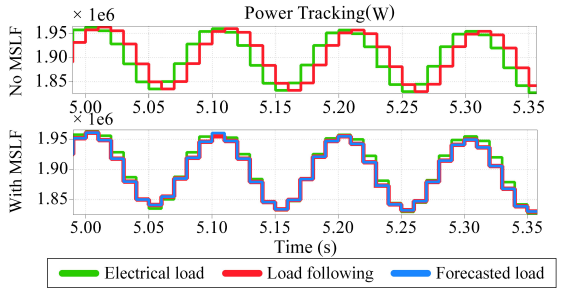

Fig. 13: Load tracking under normal load condition

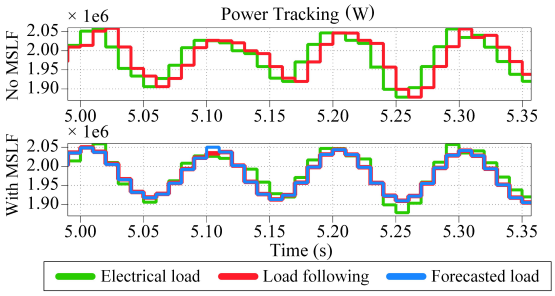

Fig. 14: Load tracking under noisy load condition

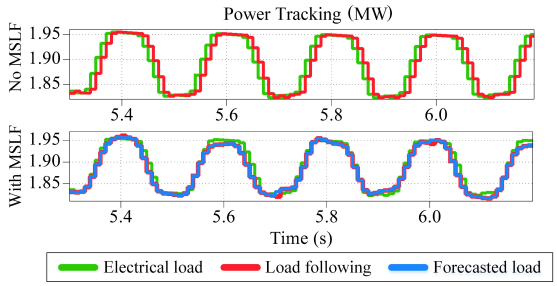

Fig. 15: Load tracking with high submergence ratio

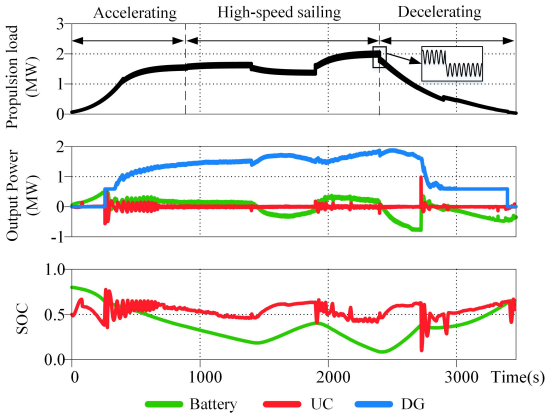

Fig. 16: Ship performance for one-hour full voyage

load is quite low and the DG is in the initial off state. Batteries supply the main load. Thereafter, DG is turned on due to the increase in load demand. From then on, both DG and HESS are in operation, with DG maintained at its optimal operating point while the batteries compensate for the lack or excess of power by delivering/taking energy. The UCs, on the other hand, support the high-frequency part. During the deceleration, the load demand decreases and the DG gradually reduces its output power, charges the batteries and is turned off at the final 2 minutes due to the low load condition.

As can be seen from the graph, the SOC of HESS is maintained at a healthy level throughout the voyage. In addition, high fuel-efficiency operation of the DG is guaranteed by the on/off scheduling at the DG controller layer and the optimal power splitting at the optimization layer. To test the fuel saving ability of the proposed PMS method, quantitative comparisons are conducted in the next subsection.

B. Fuel Savings Comparison

To evaluate the performance of the proposed PMS in terms of its fuel savings ability, several comparisons are made by comparing different diesel generator types and different PMS strategies under different load conditions. The obtained fuel consumption results for the short-time sailings are shown in

TABLE IV: Fuel consumption in short-time sailing cases when under normal load condition

DG mode	Method	Fuel consumption (kg)			
		3 knots	5 knots	5.5 knots	6.2 knots
Variable	Proposed	26.67	54.81	62.73	79.88
	LR-based	26.72	55.17	62.78	80.37
Fixed	Proposed	27.08	55.89	64.04	83.43
	LR-based	27.23	56.20	64.26	83.52

TABLE V: Fuel consumption in short-time sailing cases when under different load conditions

Load condition	MSLF	Fuel consumption (kg)			
		3 knots	5 knots	5.5 knots	6.2 knots
Normal	No	41.83	79.47	86.72	116.08
	Yes	39.89	78.13	84.78	114.67
Noisy	No	41.58	78.40	87.92	116.04
	Yes	39.94	74.84	85.98	114.02
High submergence	No	39.54	77.60	84.95	115.16
	Yes	39.54	76.86	84.93	114.23

Tab. IV and Tab. V. In these cases, the ship runs for 15 min at the speed of 3 knots (low speed), 5 knots (medium low speed), 5.5 knots (medium speed) and 6.2 knots (high speed), respectively. In Tab. IV, fixed-speed DG and the traditional LR-based method are used as benchmarks. And Tab. V gives the comparison results between the proposed PMS and the traditional ECMS without load forecasting system while under the above introduced three different sea conditions. Due to the short sailing time, these comparison results are relatively close, but it can still be observed that the proposed PMS consumes less fuel than the traditional LR-based method, especially in high ship speed. Moreover, variable-speed DG consumes less fuel than fix-speed DG. And with the integration of MSLF, the PMS has better performance than without MSLF. The reason is that MSLF provides MPC with forecasted load information in the upcoming several steps, thus guaranteeing the MPC to make wiser decisions. Compared to the traditional MPC using the same load information during its prediction horizon, MSLF integrated PMS is more suitable for fast changeable load conditions and will be more potential in fuel saving during long time sailings.

More obvious fuel savings can be obtained for long-time voyage as shown in Tab. VI, where 2.6% improvement in the fuel savings can be achieved by adopting the proposed PMS method. Besides, compared to the traditional method where the batteries are at a low SOC level at the end of the voyage (0.2), the proposed PMS maintains a high level of SOC (0.9), thus guarantee a more sufficient energy backup. Better results can be obtained with longer MPC prediction horizon as shown in Tab. VII. The results indicate better fuel saving potential and more healthy SOC with longer prediction horizon. For MPC horizon set as 15, up to 5.1% improvement in fuel saving can be achieved. However, it is worth to be noted that longer prediction horizon brings more computational efforts. Therefore the selection of the MPC predition horizon needs to be carefully decided.

To be concluded, the proposed PMS guarantees the DGs

TABLE VI: Fuel consumption

Method	Fuel consumption (kg)	Final s_{uc}	Final s_b
Proposed	206.6	0.9	0.9
LR-based	212.1	0.85	0.2

TABLE VII: Result comparison under different predict horizons

MPC N_p	Fuel consumption (kg)	Final s_{uc}	Final s_b
1	206.6	0.9	0.9
3	205.7	0.85	0.9
5	204.6	0.75	0.9
10	203.5	0.7	0.8
15	201.2	0.65	0.7

to work at high fuel efficiency point while maintaining a healthy SOC level of HESS. Considering that the cases here are only 15 minutes or one hour long, more fuel savings can be expected for longer sailing time.

C. Sensitivity Analysis

The aforementioned results are all conducted based on a certain initial states and it is assumed that all internal parameters of HESS are known. However, the changes in HESS states will have a direct influence on the power splitting and the fuel cost. To further demonstrate the effectiveness and robustness of the proposed method, sensitivity analysis is done to evaluate two key factors of HESS: the battery initial SOC, and battery charging/discharging efficiency (η_{chg} and η_{dis}). All the simulations are conducted under the one-hour full voyage load profile and the results are shown below.

1) Effects of battery initial SOC state: To test the effects of battery initial SOC state, the initial SOC is set as 20%, 30%, 40%, 50%, 60%, 70%, and 80%, respectively. The SOC variations under different initial values are shown in Fig. 17. It can be observed that the batteries can still be maintained at a healthy level even beginning from very low initial states, and can be charged to a high SOC level at the end of the voyage, thus guarantee a healthy energy backup for future cruise. In addition, the fuel consumption results under different battery SOC initial values are shown in Tab. VIII. larger initial SOC value results in less fuel consumption, which is reasonable since more energy is required to charge the battery back at the end of the voyage as seen in Fig. 17.

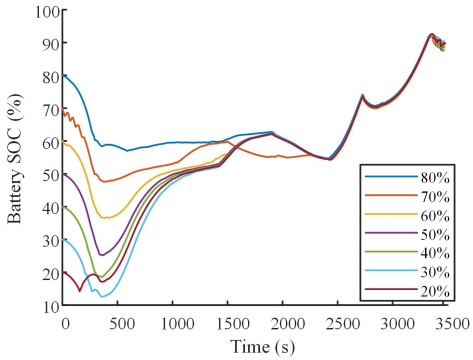

Fig. 17: Battery SOC variation under different initial SOC values

TABLE VIII: Fuel consumption under different battery SOC initials

Initial SOC (%)	80	70	60	50	40	30	20
Fuel consumption (kg)	2.052	2.085	2.095	2.115	2.14	2.161	2.217

2) Effects of battery charging and discharging efficiency: It is noted that the charging and discharging efficiency of battery varies due to degradation. The initial value of charging and discharging efficiency in the precious simulations are set as 0.95. To test the effects of their variation, 6 different cases are tested: 40%, 50%, 60%, 70%, 80%, and 90%, all based on the original value. The battery variations under these circumstances are shown in Fig. 18. And the corresponding fuel consumption is presented in Tab. IX. As seen, all batteries are maintained at a healthy level and charged to a relative high SOC state at the end of the voyage. However, the decrease in battery efficiency would discourage the charging and discharging behavior of battery and would also lead to an increase in energy consumption. Therefore, to guarantee a better energy supply, it is recommended to replace the battery with a new one for efficiencies under 80%.

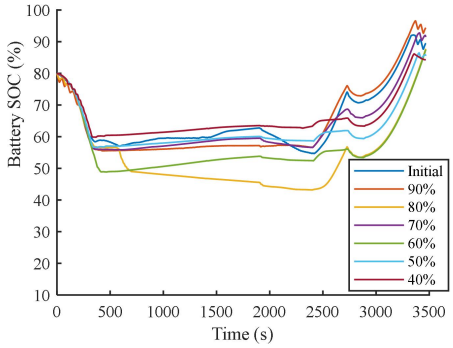

Fig. 18: Battery SOC variation under different battery charging and discharging efficiency

V. Conclusion

This paper presents a real-time power management strategy for hybrid ships, powered by hybrid energy sources (variable-speed diesel generator, batteries and ultra-capacitors). The paper aims to solve the problem of the optimal power split under highly fluctuated propulsion load with consideration of improving fuel efficiency and maintaining a healthy level of SOC throughout the voyage.

Thus, a two-layer PMS is proposed. The outer-layer is rule-based, limiting the SOC under a tolerable level by deciding the on/off status of DG. The inner-layer is optimization-based, consisting of two parallel systems: MSLF to forecast future load demand, and optimization part to decide the optimal power splitting with high DG fuel efficiency and healthy level of SOC.

Comprehensive cases including short-time sailing, long-time voyage, three extreme sea conditions, and different navigation speeds are studied. The results illustrate the effectiveness, robustness, and achievable performance of the proposed PMS strategy.

However, it is worth noting that although the ARIMA-based MSLF presented in this paper achieves good performance under different sea states, further research based on the ARIMAX model should be conducted. The major advantage of choosing ARIMA is that it relies only on past loading data, which are readily available, yet its prediction accuracy is not as good as that of ARIMAX. Given the extra information of exogenous variables (e.g. ship speed) which are pre-known, easily to be measured, and have a direct impact on the propulsion load, the accuracy can be greatly improved. Therefore, to make the idea more practical, further efforts shall be made to select the most appropriate exogenous variable after evaluating its accessibility, independence, and prediction performance. In addition, the trade-off between computational effort and accuracy will also be investigated in our future work to address the application of ARIMAX.

Acknowledgment

This work was supported by VILLUM FONDEN under the VILLUM Investigator Grant (no. 25920): Center for Research on Microgrids (CROM); www.crom.et.aau.dk

References

[1] P. Nema, R. Nema, and S. Rangnekar, "A current and future state of art development of hybrid energy system using wind and pv-solar: A review," *Renewable and Sustainable Energy Reviews*, vol. 13, no. 8, pp. 2096–2103, 2009.

[2] V. Liso, P. Xie, S. S. Araya, and J. M. Guerrero, "Modelling a modular configuration of pem fuel cell system for vessels applications," in *7TH WORLD MARITIME TECHNOLOGY CONFERENCE 2022*, 2022.

[3] J. F. Hansen, F. Wendt, and J. O. Lindtjørn, "Fuel-efficient power plant featuring variable speed generation system for dp drilling units," in *Dynamic Positioning Conference, Houston*, 2016.

[4] S. Tan, Y. Wu, P. Xie, J. M. Guerrero, J. C. Vasquez, and A. Abusorrah, "New challenges in the design of microgrid systems: Communication networks, cyberattacks, and resilience," *IEEE Electrification Magazine*, vol. 8, no. 4, pp. 98–106, 2020.

[5] P. Xie, J. M. Guerrero, S. Tan, N. Bazmohammadi, J. C. Vasquez, M. Mehrzadi, and Y. Al-Turki, "Optimization-based power and energy management system in shipboard microgrid: A review," *IEEE Systems Journal*, 2021.

[6] S. Tan, P. Xie, J. M. Guerrero, J. C. Vasquez, and R. Han, "Cyberattack detection for converter-based distributed dc microgrids: Observer-based approaches," *IEEE Industrial Electronics Magazine*, 2021.

[7] Ø. N. Smogeli, "Control of marine propellers: from normal to extreme conditions," 2006.

[8] Ø. Smogeli *et al.*, "Ventilated thrusters in dynamic positioning mode control of marine propellers from normal to extreme conditions," 2006.

[9] D. Radan, "Integrated control of marine electrical power systems," 2008.

[10] J. Hou, J. Sun, and H. Hofmann, "Control development and performance evaluation for battery/flywheel hybrid energy storage solutions to mitigate load fluctuations in all-electric ship propulsion systems," *Applied energy*, vol. 212, pp. 919–930, 2018.

[11] J. Hou, Z. Song, H. Hofmann, and J. Sun, "Adaptive model predictive control for hybrid energy storage energy management in all-electric ship microgrids," *Energy Conversion and Management*, vol. 198, p. 111929, 2019.

[12] J. Hou, Z. Song, H. Park, H. Hofmann, and J. Sun, "Implementation and evaluation of real-time model predictive control for load fluctuations mitigation in all-electric ship propulsion systems," *Applied energy*, vol. 230, pp. 62–77, 2018.

[13] J. Hou, J. Sun, and H. Hofmann, "Adaptive model predictive control with propulsion load estimation and prediction for all-electric ship energy management," *Energy*, vol. 150, pp. 877–889, 2018.

[14] P. Xie, S. Tan, J. M. Guerrero, and J. C. Vasquez, "Mpc-informed ecms based real-time power management strategy for hybrid electric ship," *Energy Reports*, vol. 7, pp. 126–133, 2021.

TABLE IX: Fuel consumption under different battery charging and discharging efficiency

Initial SOC (%)	initial	90	80	70	60	50	40
Fuel consumption (kg)	2.052	2.054	2.059	2.062	2.073	2.085	2.087

[15] Z. Zhang, C. Guan, and Z. Liu, "Real-time optimization energy management strategy for fuel cell hybrid ships considering power sources degradation," *IEEE Access*, vol. 8, pp. 87 046–87 059, 2020.

[16] P. Xie, S. Tan, N. Bazmohammadi, J. M. Guerrero, J. C. Vasquez, J. M. Alcala, and J. E. M. Carreño, "A distributed real-time power management scheme for shipboard zonal multi-microgrid system," *Applied Energy*, vol. 317, p. 119072, 2022.

[17] M. Kunicka and W. Litwin, "Energy demand of short-range inland ferry with series hybrid propulsion depending on the navigation strategy," *Energies*, vol. 12, no. 18, p. 3499, 2019.

[18] F. Baldi, F. Ahlgren, T.-V. Nguyen, M. Thern, and K. Andersson, "Energy and exergy analysis of a cruise ship," *Energies*, vol. 11, no. 10, p. 2508, 2018.

[19] L. Maharjan, S. Inoue, H. Akagi, and J. Asakura, "State-of-charge (soc)-balancing control of a battery energy storage system based on a cascade pwm converter," *IEEE Transactions on Power Electronics*, vol. 24, no. 6, pp. 1628–1636, 2009.

[20] N. Amjady, F. Keynia, and H. Zareipour, "Short-term load forecast of microgrids by a new bilevel prediction strategy," *IEEE Transactions on smart grid*, vol. 1, no. 3, pp. 286–294, 2010.

[21] Z. Li, Y. Xu, S. Fang, X. Zheng, and X. Feng, "Robust coordination of a hybrid ac/dc multi-energy ship microgrid with flexible voyage and thermal loads," *IEEE Transactions on Smart Grid*, vol. 11, no. 4, pp. 2782–2793, 2020.

[22] D. Gao, X. Wang, T. Wang, Y. Wang, and X. Xu, "An energy optimization strategy for hybrid power ships under load uncertainty based on load power prediction and improved nsga-ii algorithm," *Energies*, vol. 11, no. 7, p. 1699, 2018.

[23] S. Mashayekh and K. L. Butler-Purry, "An integrated security-constrained model-based dynamic power management approach for isolated microgrids in all-electric ships," *IEEE Transactions on Power Systems*, vol. 30, no. 6, pp. 2934–2945, 2015.

[24] M. Mehrzadi, Y. Terriche, C.-L. Su, P. Xie, N. Bazmohammadi, M. N. Costa, C.-H. Liao, J. C. Vasquez, and J. M. Guerrero, "A deep learning method for short-term dynamic positioning load forecasting in maritime microgrids," *Applied Sciences*, vol. 10, no. 14, p. 4889, 2020.

[25] K. Wang, X. Yan, Y. Yuan, X. Jiang, X. Lin, and R. R. Negenborn, "Dynamic optimization of ship energy efficiency considering time-varying environmental factors," *Transportation Research Part D: Transport and Environment*, vol. 62, pp. 685–698, 2018.

[26] R. Tang, Z. Wu, and X. Li, "Optimal operation of photovoltaic/battery/diesel/cold-ironing hybrid energy system for maritime application," *Energy*, vol. 162, pp. 697–714, 2018.

[27] H. Park, J. Sun, S. Pekarek, P. Stone, D. Opila, R. Meyer, I. Kolmanovsky, and R. DeCarlo, "Real-time model predictive control for shipboard power management using the ipa-sqp approach," *IEEE Transactions on Control Systems Technology*, vol. 23, no. 6, pp. 2129–2143, 2015.

[28] F. D. Kanellos, A. Anvari-Moghaddam, and J. M. Guerrero, "A cost-effective and emission-aware power management system for ships with integrated full electric propulsion," *Electric Power Systems Research*, vol. 150, pp. 63–75, 2017.

[29] Z. Wu and X. Xia, "Tariff-driven demand side management of green ship," *Solar Energy*, vol. 170, pp. 991–1000, 2018.

[30] A. Haseltalab and R. R. Negenborn, "Model predictive maneuvering control and energy management for all-electric autonomous ships," *Applied Energy*, vol. 251, p. 113308, 2019.

[31] J. Hou, J. Sun, and H. Hofmann, "Adaptive model predictive control with propulsion load estimation and prediction for all-electric ship energy management," *Energy*, vol. 150, pp. 877–889, 2018.

[32] J. Hou, J. Sun, and H. F. Hofmann, "Mitigating power fluctuations in electric ship propulsion with hybrid energy storage system: Design and analysis," *IEEE Journal of Oceanic Engineering*, vol. 43, no. 1, pp. 93–107, 2017.

[33] I. Kolmanovsky, I. Sivergina, and J. Sun, "Simultaneous input and parameter estimation with input observers and set-membership parameter bounding: theory and an automotive application," *International Journal of Adaptive Control and Signal Processing*, vol. 20, no. 5, pp. 225–246, 2006.

[34] P. Wu, J. Partridge, and R. Bucknall, "Cost-effective reinforcement learning energy management for plug-in hybrid fuel cell and battery ships," *Applied Energy*, vol. 275, p. 115258, 2020.

[35] Z. Deng, B. Wang, Y. Xu, T. Xu, C. Liu, and Z. Zhu, "Multi-scale convolutional neural network with time-cognition for multi-step short-term load forecasting," *IEEE Access*, vol. 7, pp. 88 058–88 071, 2019.

[36] J.-P. Jalkanen, L. Johansson, J. Kukkonen, A. Brink, J. Kalli, and T. Stipa, "Extension of an assessment model of ship traffic exhaust emissions for particulate matter and carbon monoxide," *Atmospheric Chemistry and Physics*, vol. 12, no. 5, pp. 2641–2659, 2012.

[37] K. Satpathi, V. M. Balijepalli, and A. Ukil, "Modeling and real-time scheduling of dc platform supply vessel for fuel efficient operation," *IEEE Transactions on Transportation Electrification*, vol. 3, no. 3, pp. 762–778, 2017.

[38] K. R. Wheeler, "Efficient operation of diesel generator sets in remote conditions," Ph.D. dissertation, Virginia Tech, 2017.

[39] W. Zhang, J. Li, L. Xu, and M. Ouyang, "Optimization for a fuel cell/battery/capacity tram with equivalent consumption minimization strategy," *Energy Conversion and Management*, vol. 134, pp. 59–69, 2017.

[40] K. R. Wheeler, "Efficient operation of diesel generator sets in remote conditions," Ph.D. dissertation, Virginia Tech, 2017.

[41] M. M. Barnitsas, D. Ray, and P. Kinley, "Kt, kq and efficiency curves for the wageningen b-series propellers," University of Michigan, Tech. Rep., 1981.

[42] K. J. Minsaas, O. M. Faltinsen, and B. Persson, "On the importance of added resistance, propeller immersion and propeller ventilation for large ships in a seaway," 1983.

[43] A. Sciarretta, L. Serrao, P. Dewangan, P. Tona, E. Bergshoeff, C. Bordons, L. Charmpa, P. Elbert, L. Eriksson, T. Hofman *et al.*, "A control benchmark on the energy management of a plug-in hybrid electric vehicle," *Control engineering practice*, vol. 29, pp. 287–298, 2014.

[44] M. Kalikatzarakis, R. Geertsma, E. Boonen, K. Visser, and R. Negenborn, "Ship energy management for hybrid propulsion and power supply with shore charging," *Control Engineering Practice*, vol. 76, pp. 133–154, 2018.

[45] L. W. Chua, T. Tjahjowidodo, G. G. Seet, and R. Chan, "Implementation of optimization-based power management for all-electric hybrid vessels," *IEEE Access*, vol. 6, pp. 74 339–74 354, 2018.

[46] Z. Hong, Q. Li, Y. Han, W. Shang, Y. Zhu, and W. Chen, "An energy management strategy based on dynamic power factor for fuel cell/battery hybrid locomotive," *International Journal of Hydrogen Energy*, vol. 43, no. 6, pp. 3261–3272, 2018.

[47] V. Kotu and B. Deshpande, *Data science: concepts and practice*. Morgan Kaufmann, 2018.

[48] H. Akaike, "Fitting autoregressive models for prediction," *Annals of the institute of Statistical Mathematics*, vol. 21, no. 1, pp. 243–247, 1969.

[49] E. Ruth, "Propulsion control and thrust allocation on marine vessels," 2008.

[50] J. Bakkeheim, T. A. Johansen, Ø. N. Smogeli, and A. J. Sorensen, "Lyapunov-based integrator resetting with application to marine thruster control," *IEEE Transactions on Control Systems Technology*, vol. 16, no. 5, pp. 908–917, 2008.

[51] C. A. M. Vásquez, "Evaluation of medium speed diesel generator sets and energy storage technologies as alternatives for reducing fuel consumption and exhaust emissions in electric propulsion systems for psvs," *Ciencia y tecnología de buques*, vol. 9, no. 18, pp. 49–62, 2016.

Peilin Xie (S'19) received the B.S. degree in Electrical Engineering from Beijing Jiaotong University, Beijing, China in 2015, and the M.S. degree in Electrical Engineering and Automation from North China Electric Power University, Beijing, China, in 2018. She is currently working toward her Ph.D. degree with the Department of Energy Technology, Aalborg University, Aalborg, Denmark.

Her research mainly include virtual synchronous generator technology, the power management control for shipboard microgrids, and distributed PMS for large-scale shipboard microgrids.

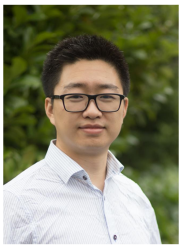

Sen Tan (S'20) received the B.S. degree in Automation, the M.S. degree in Control Engineering both from Northeastern University, Liaoning, China, in 2014 and 2017 respectively. He is currently pursuing the Ph.D. degree with the Department of Energy Technology, Aalborg University, Denmark.

His research interests include distributed control and power management strategy design for microgrid, fault detection and motor drive technologies.

Najmeh Bazmohammadi received the bachelor's degree in electrical engineering and the master's degree in electrical engineering-Control from the Ferdowsi University of Mashhad, Iran in 2009 and 2012, respectively and the Ph.D. degree in electrical engineering-Control from the K. N. Toosi University of Technology, Tehran, Iran in 2019. She is currently a postdoctoral research fellow with the Center for Research on Microgrids (CROM), Department of Energy Technology, Aalborg University, Denmark.

Her current research interests include modeling and control of dynamic systems, decision-making under uncertainty, model predictive control and its application in energy management of hybrid and renewable-based power systems and life support systems.

Josep M. Guerrero (S'01-M'04-SM'08-FM'15) received the B.S. degree in telecommunications engineering, the M.S. degree in electronics engineering, and the Ph.D. degree in power electronics from the Technical University of Catalonia, Barcelona, in 1997, 2000 and 2003, respectively. Since 2011, he has been a Full Professor with the Department of Energy Technology, Aalborg University, Denmark, where he is responsible for the Microgrid Research Program. From 2014 he is chair Professor in Shandong University; from 2015 he is a distinguished guest Professor in Hunan University; and from 2016 he is a visiting professor fellow at Aston University, UK, and a guest Professor at the Nanjing University of Posts and Telecommunications. From 2019, he became a Villum Investigator by The Villum Fonden, which supports the Center for Research on Microgrids (CROM) at Aalborg University, being Prof. Guerrero the founder and Director of the same centre (www.crom.et.aau.dk).

His research interests is oriented to different microgrid aspects, including power electronics, distributed energy-storage systems, hierarchical and cooperative control, energy management systems, smart metering and the internet of things for AC/DC microgrid clusters and islanded minigrids. Specially focused on microgrid technologies applied to offshore wind, maritime microgrids for electrical ships, vessels, ferries and seaports, and space microgrids applied to nanosatellites and spacecrafts. Prof. Guerrero is an Associate Editor for a number of IEEE TRANSACTIONS. He has published more than 500 journal papers in the fields of microgrids and renewable energy systems, which are cited more than 50,000 times. He received the best paper award of the IEEE Transactions on Energy Conversion for the period 2014-2015, and the best paper prize of IEEE-PES in 2015. As well, he received the best paper award of the Journal of Power Electronics in 2016. During six consecutive years, from 2014 to 2019, he was awarded by Clarivate Analytics (former Thomson Reuters) as Highly Cited Researcher. In 2015 he was elevated as IEEE Fellow for his contributions on "distributed power systems and microgrids."

Juan C. Vasquez (M'12-SM'14) received the B.S. degree in electronics engineering from the Autonomous University of Manizales, Manizales, Colombia, and the Ph.D. degree in automatic control, robotics, and computer vision from BarcelonaTech-UPC, Spain, in 2004 and 2009, respectively. In 2011, He was Assistant Professor and in 2014, Associate Professor at the Department of Energy Technology, Aalborg University, Denmark. In 2019, He became Professor in Energy Internet and Microgrids and currently He is the Co-Director of the Villum Center for Research on Microgrids (see crom.et.aau.dk). He was a Visiting Scholar at the Center of Power Electronics Systems (CPES) at Virginia Tech, USA and a visiting professor at Ritsumeikan University, Japan. His current research interests include operation, advanced hierarchical and cooperative control, optimization and energy management applied to distributed generation in AC/DC Microgrids, maritime microgrids, advanced metering infrastructures and the integration of Internet of Things and Energy Internet into the SmartGrid. Prof.Vasquez is an Associate Editor of IET POWER ELECTRONICS and a Guest Editor of the IEEE TRANSACTIONS ON INDUSTRIAL INFORMATICS Special Issue on Energy Internet. Prof. Vasquez was awarded as Highly Cited Researcher by Thomson Reuters from 2017 to 2019 and He was the recipient of the Young Investigator Award 2019. He has published more than 450 journal papers in the field of Microgrids, which in total are cited more than 19000 times. Dr. Vasquez is currently a member of the IEC System Evaluation Group SEG4 on LVDC Distribution and Safety for use in Developed and Developing Economies, the Renewable Energy Systems Technical Committee TC-RES in IEEE Industrial Electronics, PELS, IAS, and PES Societies.